ELSEVIER

Journal of Molecular Catalysis A: Chemical 180 (2002) 67–76

JOURNAL OF MOLECULAR CATALYSIS A: CHEMICAL

www.elsevier.com/locate/molcata

A new class of ruthenium complexes containing Schiff base ligands as promising catalysts for atom transfer radical polymerization and ring opening metathesis polymerization

Bob De Clercq, Francis Verpoort*

Department of Inorganic and Physical Chemistry, Ghent University, Krijgslaan 281 (S-3), 9000 Gent, Belgium

Received 15 August 2001; accepted 12 November 2001

Abstract

A novel series of Schiff base ruthenium complexes that are active catalysts in the field of atom transfer radical polymerization (ATRP), have been prepared. Moreover, when activated with trimethylsilyldiazomethane (TMSD), these species exhibit good catalytic activity in the ring opening metathesis polymerization (ROMP) of norbornene and cyclooctene. The activity for both the ROMP and ATRP reaction is dependent on the steric bulk and electron donating ability of the Schiff base ligand. The control over polymerization in ATRP was verified for the two substrates that exhibit the highest activity, namely MMA and styrene. The results show that the optimal ATRP equilibrium leading to a controlled polymerization, can be established by adjusting the steric and electronic properties of the Schiff base ligand. © 2002 Elsevier Science B.V. All rights reserved.

Keywords: Ring opening metathesis polymerization; Atom transfer radical polymerization; Ruthenium alkylidene; Schiff bases; Homogeneous catalysis

1. Introduction

Well-defined polymers with low polydispersities (PDI) and complex architectures can be achieved by living polymerization processes in which there is neither chain transfer nor termination. Before the mid 90’s, most of the living polymerization systems were reported for anionic [1], cationic [2] or group transfer polymerizations [3]. However, the industrial applications of these techniques have been limited by the need for high-purity monomers and solvents, reactive initiators and anhydrous conditions. In contrast, free radical polymerization is probably the most important commercial process leading to high molecular weight polymers. A large variety of monomers can be polymerised and copolymerised radically under relatively simple experimental conditions which require the absence of oxygen but can be carried out in the presence of water. However, free radical polymerization processes often yield polymers with ill-controlled molecular weights and high polydispersities. The idea of combining the advantages of both living polymerization and radical polymerization has attracted much attention. Indeed, recent years have witnessed a rapid progress in the development of controlled/“living” radical polymerization. Among the newly introduced controlled radical polymerization processes, atom transfer radical polymerization (ATRP) is most successful. The groups of Kato et al. [4], and Wang and Matyjaszewski [5] reported in 1995 on this living radical polymerization process. ATRP is based on a

---

* Corresponding author. Tel.: +32-9-264-44-36; fax: +32-9-264-49-83.
E-mail addresses: b.declercq@rug.ac.be (B. De Clercq), francis.verpoort@rug.ac.be (F. Verpoort).

PII: S1381-1169(01)00451-4

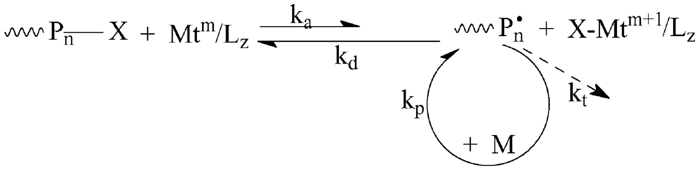

Scheme 1. Atom transfer radical polymerization (ATRP) (M: monomer, Mt: metal).

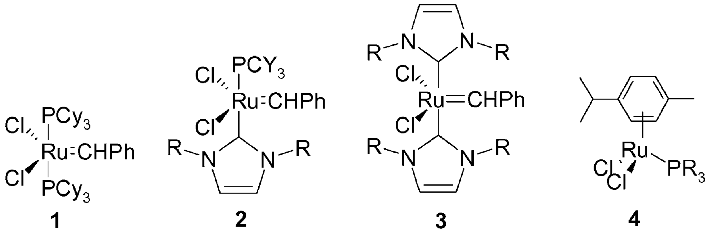

Fig. 1. Catalyst that are efficient for both olefin metathesis and ATRP reactions.

dynamic equilibration between the propagating radicals and the dormant species which is established through the reversible transition metal-catalysed cleavage of the covalent carbon–halogen bond in the dormant species (Scheme 1).

Polymerization systems utilising this concept have been developed with complexes of Cu, Ru, Ni, Pd, Rh and Fe to establish the ATRP equilibrium [6].

Recently, there have been some reports on the ATRP activity of the complexes **1**, **2**, **3** and **4** (Fig. 1) [7]. The complexes **1**, **2** and **3** are also known to be highly efficient for ring opening metathesis polymerization (ROMP) reactions [8] and when activated with trimethylsilyldiazomethane (TMSD) also **4** shows high activity for ROMP reactions [9].

The dual behaviour of these ruthenium catalysts prompted us to explore the activity of some new homogeneous catalytic ruthenium-based systems in the field of ATRP and ROMP.

2. Results and discussion

2.1. Synthesis

2.1.1. General procedure for the preparation of Schiff base ligands

The condensation of salicylaldehyde with the aromatic amine derivative was carried out with stirring in ethanol (p.a.) at 80 °C for 2 h. Upon cooling to 0 °C, a yellow solid precipitated from the reaction mixture. The solid was filtered, washed with cold ethanol and then dried in vacuo to afford the desired salicylaldimine ligand in excellent yields. The condensation of salicylaldehyde with the aliphatic amine derivatives was carried out with stirring in THF at reflux temperature for 2 h. The reaction mixture changed from a colourless to a yellow solution and was further used without purification (Scheme 2).

2.1.2. General procedure for the preparation of thallium salts ***2-a***, ***2-b***, ***2-c***

To a solution of Schiff bases **1-a**, **1-b**, **1-c** in THF (15 ml) was added drop-wise a solution of thalliumethoxide in THF (5 ml) at room temperature. Immediately after the addition, a yellow solid formed and the reaction mixture was stirred for 2 h at room temperature. Filtration of the solid under a nitrogen atmosphere gave the thallium salts **2-a**, **2-b**, **2-c** in quantitative yields. The salts were immediately used in the next step without further purification.

2.1.3. General procedure for the preparation of Schiff base substituted Ru complexes ***3-a***, ***3-b***, ***3-c***

To a solution of $[RuCl_2(p\text{-cymene})]_2$ in THF (5 ml) was added a solution of the corresponding thallium salts in THF (5 ml). The reaction mixture was stirred at room temperature for 6 h. The thalliumchloride

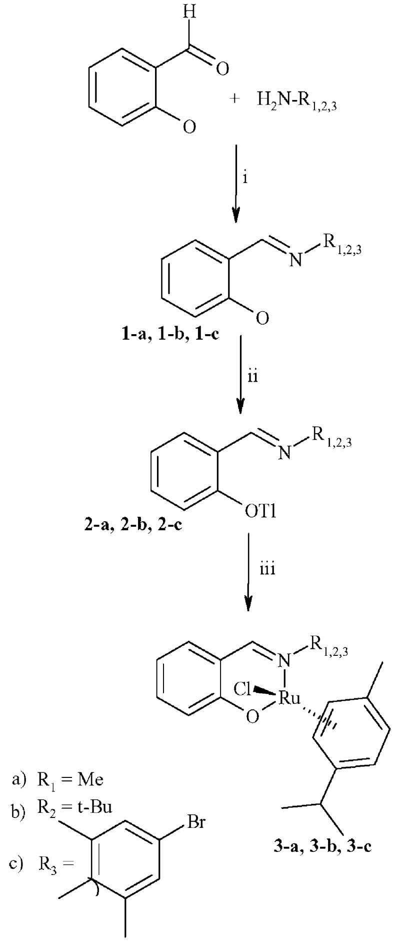

Scheme 2. Reaction sequence for the synthesis of the three different Schiff base substituted ruthenium catalysts (i) THF, Δ, 2 h for $H_2NR_{1,2}$ and EtOH, 80 °C, 2 h for H_2NR_3; (ii) TlOEt, THF, RT, 2 h; (iii) $[RuCl_2(p\text{-cymene})]_2$, THF, RT, 6 h.

(the by-product of the reaction) was removed via filtration. After evaporation of the solvent, the residue was dissolved in a minimal amount of toluene and cooled to 0 °C. The obtained crystals were then washed with cold toluene (3 × 10 ml) and dried. The Schiff base ruthenium complexes **3-a**, **3-b**, **3-c** appeared as red-brown solids.

The percentage conversion versus time plot for the ROMP of norbornene and cyclooctene are depicted in Figs. 2 and 3, respectively. The properties of the polyNBE and polycyclooctene obtained with the different catalytic systems are summarised in Tables 1 and 2, respectively.

Table 1
Properties of the polyNBE formed with the catalytic systems **3-a**, **3-b** and **3-c** when activated with a catalytic amount of TMSD

	M_n	M_w	PDI	*cis*/*trans*
3-a	74000	471000	6.34	0.38
3-b	78000	462000	5.95	0.32
3-c	98000	682000	6.95	0.39

Table 2
Properties of the polycyclooctene formed with the catalytic systems **3-a**, **3-b** and **3-c** when activated with a catalytic amount of TMSD

	M_n	M_w	PDI	*cis*/*trans*
3-c	57000	262000	4.62	0.38
3-a	55000	181000	3.26	0.36
3-b	59000	196000	3.35	0.34

For both ROMP reactions of NBE and cyclooctene, a linear increase of the conversion versus time is observed within the time period of 80 min. After this period, for all three systems the maximum conversion for both NBE and cyclooctene polymerization is reached. The catalytic system with the aromatic substituted imine ligand (**3-c**) is clearly the most active. The polydispersities are in all cases broad which indicates that the polymerization is subjected to backbiting and transfer reactions.

A *trans* configuration of the polyNBE and polycyclooctene is preferred. This is in accordance with the general observation for ruthenium catalysts in ROMP reactions [8].

When the polymerization of norbornene was tested with pure TMSD (no addition of catalyst, 1 ml of a 0.8410 M NBE solution in toluene and [NBE]/[TMSD] = 800/2, tested at 85 and 40 °C, 6 h) no polymerization was observed. However, when norbornene was tested with the homogeneous catalyst **3-c** without activation with TMSD ([Ru]/[NBE] = 1/800, 1 ml toluene, 6 h), a conversion of 6% was observed. Because there was no TMSD activation, the initiating metal–carbene complex must result from a reaction between the catalyst and the substrate olefin.

In order to elucidate the mechanism of carbene formation, 0.5 mmol of the catalyst solution in C_6D_6 was transferred into a 15 ml vessel followed by the addition of 1 equivalent of norbornene solution in C_6D_6. The reaction mixture was then heated for 4 h

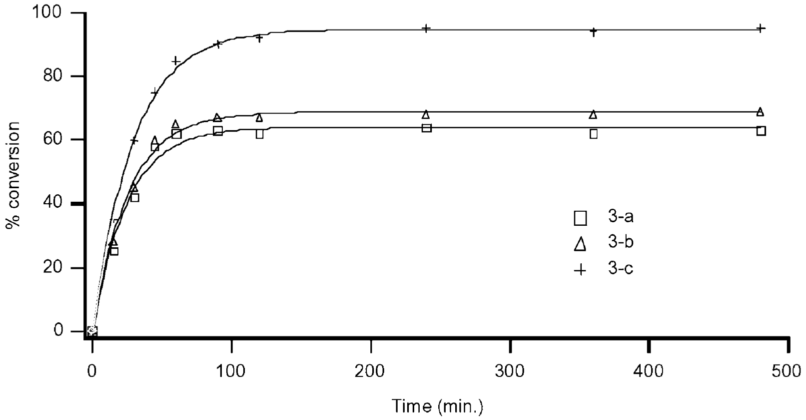

Fig. 2. Plot of the percentage conversion vs. time for the ROMP of norbornene using catalysts **3-a**, **3-b** and **3-c**.

at 85 °C. After cooling to RT the reaction mixture was quenched with 10 equivalents ethylvinylether. ^{1}H-NMR of the reaction mixture revealed the presence of a species containing the alkoxy substituted carbene ligand [Ru] = CHOEt (compound **3**, Scheme 3). The proton of this species is absorbed at 14.95 ppm as a singlet. After purification of the concentrated reaction mixture by flash column chromatography using silica gel, the methylene–norbornane compound (compound **4**, Scheme 3) was unambiguously identified by ^{1}H-NMR and ^{13}C-NMR analysis. When a reaction mixture of 0.5 mmol of the catalyst solution in C_6D_6 and 5 equivalents of norbornene solution in C_6D_6 was stirred for 4 h at 85 °C, the propagating carbene proton of the polymer growing chain (compound **5**, Scheme 3) appeared as a doublet at 18.85 ppm. Despite careful NMR monitoring, no evidence was found for a η^4 or η^2 ligation of the *p*-cymene ligand. Moreover, the ^{1}H-NMR measurements reveal that the propagating ruthenium–carbene peak could be integrated for about 2.5% of the total ruthenium in solution, in agreement with the amount of free *p*-cymene released in the solution.

These results strongly support the assumption that the homogeneous catalyst, which is an 18-electron complex, catalyses the polymerization of norbornene, through the loss of a *p*-cymene ligand followed by coordination of the norbornene and rearrangement to a ruthenium–carbene complex which then propagates ROMP. Therefore, it is very reasonable to assume that compound **2** from Scheme 3, produced by a 2,3 hydrogen shift in the ruthenium–olefin complex

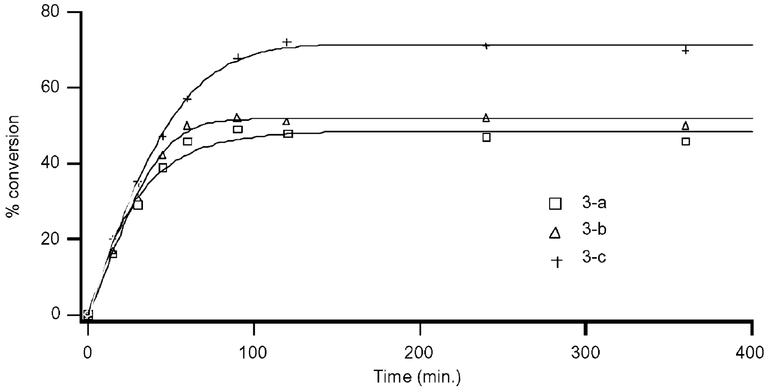

Fig. 3. Plot of the percentage conversion vs. time for the ROMP of cyclooctene using catalysts **3-a**, **3-b** and **3-c**.

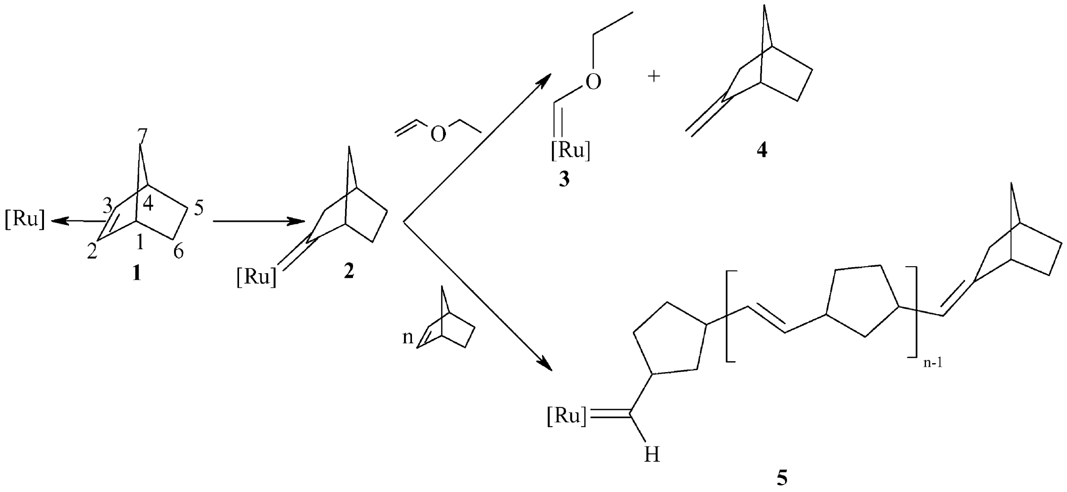

Scheme 3. Possible mechanism for the formation of the initial metal–carbene in the absence of TMSD.

(compound **1** from Scheme 3), is here the initiating ruthenium–carbene complex.

When 2 equivalents TMSD were added to a solution containing 0.5 mmol of catalytic system **3-c** in C_6D_6, evolution of nitrogen took place and a species containing the trimethylsilyl-substituted carbene ligand, $[Ru] = CHSiMe_3$, was observed in ^{1}H-NMR (in the absence of olefin). The proton of this carbene species absorbed at 23.66 ppm as a singlet and the methyl groups of the carbene–trimethylsilyl moiety appeared as a singlet at 0.46 ppm at room temperature. As soon as norbornene (5 equivalents in C_6D_6) was added to the reaction mixture, the species at 23.66 ppm vanished and was replaced by the propagating carbene of the growing polymer chain at 18.85 ppm. Now, the ruthenium–carbene peak could be integrated for about 12% of the total ruthenium in solution, again in agreement with the amount of free *p*-cymene released in solution after addition of TMSD. Again, no η^4 or η^2 ligation of the arene ligand was observed during ^{1}H-NMR monitoring of the reaction mixture. Moreover, studies by other teams dealing with metathesis reactions mediated by ruthenium–arene complexes have shown that the release of the arene ligand is crucial and is responsible for the generation of the catalytically active species [7,10,13]. Therefore, it is plausible to state that the mechanism depicted in Scheme 4 is responsible for the formation of the catalytically active species in ROMP reactions with **3-a**, **3-b** and **3-c** activated with TMSD.

In Table 3 polymer yields obtained with these catalytic systems for ATRP reactions are summarised.

Here also catalyst **3-c** gives the highest conversions. For methylmethacrylate (entry 3) and styrene (entry 6) almost quantitative conversions are obtained. Comparing the catalytic activity of the different systems towards the polymerization of acrylates and methacrylates, it is obvious that the methacrylates (entries 3 and 4) are polymerised more easily than the acrylates (entries 1 and 2). For both the acrylates and methacrylates, the conversion decreases when the substrate becomes too bulky (compare entry 2 and 1 for the acrylates and entry 4 and 3 for the methacrylates). Unfortunately, the catalysts were not able to polymerise acrylonitrile.

The properties of the polymers obtained with styrene and methylmethacrylate (MMA), the two substrates which give the highest conversions, are depicted in Table 4. For the systems **3-a** and **3-b** the quite broad polydispersities indicate a less controlled polymerization.

However, for system **3-c**, the good initiator efficiencies and the polydispersities obtained, indicate that the polymerization proceeds in a more restrained fashion.

Moreover, the linear time dependence of $\ln([M]_0/[M]_t)$ (Fig. 4) and the linear relationship between M_n and the conversion (Fig. 5) for both styrene and MMA

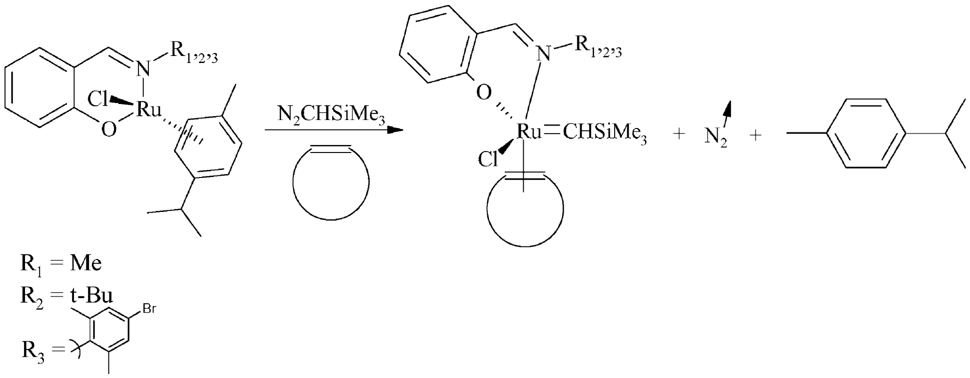

Scheme 4. Possible mechanism for the formation of the catalytically active species in ROMP reactions.

Table 3
ATRP results of representative substrates (T = 85 °C except for styrene 110 °C and acrylonitrile 65 °C, solvent: toluene, [substrate]/[catalyst]/[initiator] = 800/1/2, NR: no reaction)

Entry	Substrate	Initiator	Time (min)	**3-a** (%)	**3-b** (%)	**3-c** (%)
1	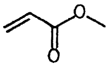	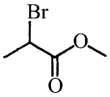	60	6	7	11
			480	35	45	52
			1020	34	46	54
2	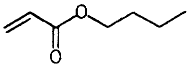		60	6	10	9
			480	16	22	34
			1020	19	24	35
3	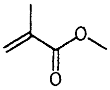	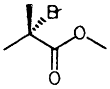	60	19	26	22
			480	66	77	84
			1020	66	76	84
4	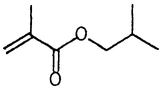		60	7	8	13
			480	35	38	58
			1020	34	39	62
5	$H_2C{=}CHCN$	$H_3C–CH(Cl)CN$	60			
			480	NR	NR	NR
			1020			
6	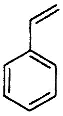	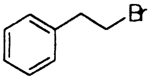	60	19	36	48
			480	69	75	93
			1020	74	77	95

Table 4
Properties of the polymers formed via ATRP

	Styrene/*methylmethacrylate*[a]			
	M_n[b]	M_w[b]	PDI[b]	f_i[c]
3-a	40000/*34000*	84000/*67000*	2.10/*1.97*	0.70/*0.64*
3-b	38000/*39000*	74000/*79000*	1.94/*2.01*	0.61/*0.63*
3-c	54000/*48000*	98000/*84000*	1.81/*1.75*	0.70/*0.71*

[a] Properties determined of polymers obtained after 8 h of reaction.

[b] GPC versus polystyrene standards.

[c] f_i = initiator efficiency = $M_{n(\text{theor.})}/M_{n(\text{exp.})}$ with $M_{n(\text{theor.})}$ = ([monomer]$_0$/[initiator]$_0$) × MW_{monomer} × conversion.

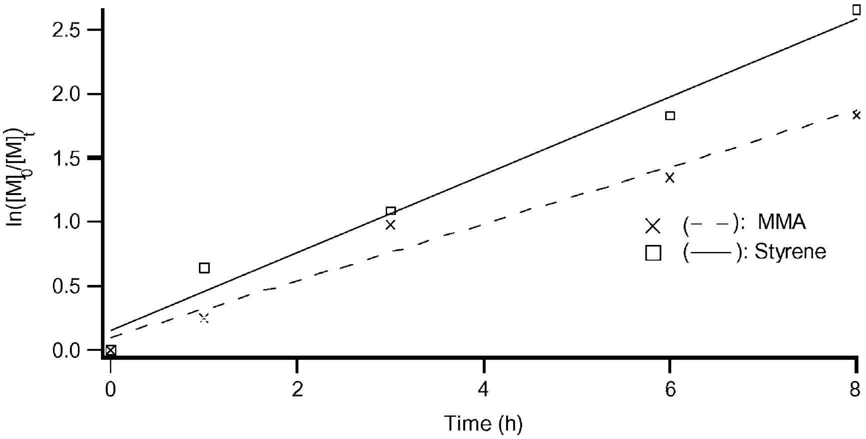

Fig. 4. Plot of ln([M]$_0$/[M]$_t$) vs. time (h) for MMA and styrene polymerization mediated by complex **3-c** at 85 and 110 °C, respectively. [M]$_0$ and [M]$_t$ are the monomer concentrations at times 0 and t, respectively.

with catalyst **3-c** is also in agreement with a controlled process with a constant number of growing chains. Also, the observation that the polydispersities decrease with increasing conversion is in agreement with a controlled polymerization following the ATRP concept (Fig. 6).

The reason for the difference in control over polymerization must be sought in the lability of the X–Mt bond in the deactivator [11] which increases in the order of **3-a** < **3-b** < **3-c**. To get an idea of the lability of the Mt–X bond, the atomic charge on the nitrogen atom of the Schiff base ligands was deducted by modelling these compounds via a semi-empirical molecular orbital method [12]. The atomic charges were −0.099718, −0.172322 and −0.511666 e (with $1\ e = 1.6021 \times 10^{-19}$ C) for compounds **3-a**, **3-b** and **3-c**, respectively. It is obvious that the more electron donating the N of the Schiff base becomes, the more the lability of the Mt–X bond increases.

These results support the idea that control over polymerization in ATRP with catalysts **3-a**, **3-b** and **3-c** can easily be improved by fine-tuning the Schiff base ligands in order to find the ideal Mt–X bond strength leading to the optimal ATRP equilibrium.

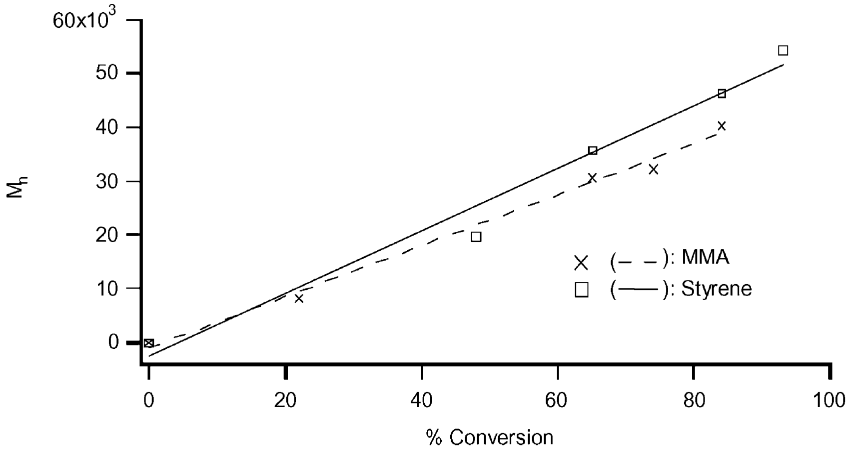

Fig. 5. Plot of M_n vs. the percentage conversion for MMA and styrene polymerization mediated by complex **3-c** at 85 and 110 °C, respectively.

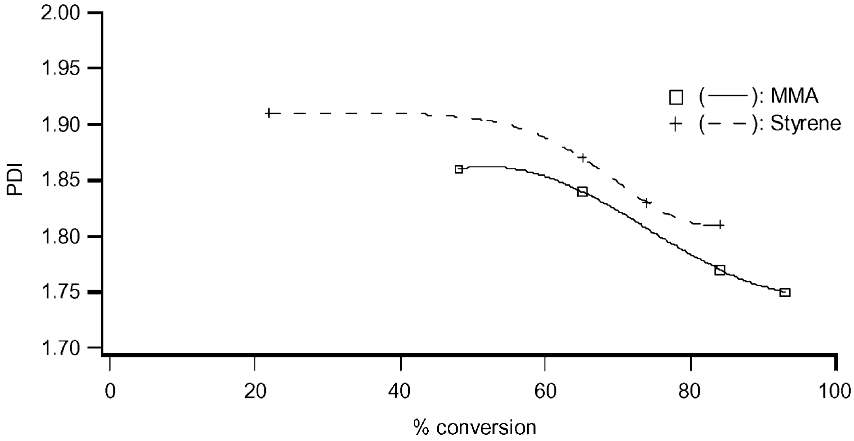

Fig. 6. Evolution of polydispersities with percentage conversion for MMA and styrene polymerization mediated by complex **3-c**.

The observation that the activity of our systems improve with increasing bulkiness of the Schiff base ligand (compare the results of catalysts **3-a** and **3-b**) and increasing negative atomic charge on the N atom of the Schiff base ligand, follows the same trend that Demonceau and coworkers found with their $RuPR_3Cl_2$(*p*-cymene) systems where an increased activity towards ATRP and ROMP reactions was witnessed as the bulkiness and the basicity of the phosphine ligands increased [9,14].

3. Experimental section

3.1. General

All reactions and manipulations were performed under an argon atmosphere by using conventional Schlenck-tube techniques. Argon gas was dried by passage through P_2O_5 (Aldrich 97%). ^{1}H-NMR (500 MHz) and ^{13}C-NMR (126 MHz) spectra were recorded on a Bruker AM spectrometer. IR spectra were taken with a Mattson 5000 FTIR spectrometer. The number and weight average molecular weights (M_n and M_w) and polydispersity (M_w/M_n) of the polymers were determined by gel permeation chromatography ($CHCl_3$, 25 °C) using polystyrene standards. The GPC instrument used is a Waters Maxima 820 system equipped with a PL gel column.

The ruthenium dimer $[RuCl_2(p\text{-cymene})]_2$ was prepared according to literature procedures [15] and the structure and purity was checked with IR and ^{1}H-NMR spectroscopy. Cyclooctene and norbornene were purchased from Aldrich and distilled from CaH_2 under nitrogen prior to use. Commercial grade solvents were dried and deoxygenated for at least 24 h over appropriate drying agents under nitrogen atmosphere and distilled prior to use. Unless otherwise noted, all other compounds were purchased from Aldrich, and used as received.

In a typical ROMP experiment 0.005 mmol of the catalyst solution in toluene was transferred into a 15 ml vessel followed by the addition of a catalytic amount (2 equivalents) of TMSD diluted in 1 ml toluene via a precision syringe over 0.5 h to allow the formation of the initiating metal–carbene species. Then, the right amount of monomer solution in toluene (800 equivalents for norbornene, 200 equivalents for cyclooctene) was added and the reaction mixture was then kept stirring at 85 °C for different time periods. To stop the polymerization reaction, 2–3 ml of an ethylvinylether/BHT solution is added and the solution is stirred till the deactivation of the active species is completed. The solution is poured into 50 ml methanol (containing 0.1% BHT) and the polymers are precipitated and dried in vacuum overnight.

In a typical ATRP experiment 0.0117 mmol of catalyst was placed in a glass tube (in which the air was expelled by three vacuum–nitrogen cycles) containing a magnet barr and capped by a three-way stopcock. Then, the monomer and initiator were added so that the molar ratios [catalyst]/[initiator]/[monomer] were

1/2/800. All liquids were handled under argon with dried syringes. The reaction mixture was then heated for different time periods at the reaction temperature which was 85 °C for the acrylates and methacrylates, 110 °C for styrene and 65 °C for acrylonitrile. After cooling, it was diluted in THF and poured in 50 ml *n*-heptane (for the acrylates, methacrylates and acrylonitrile) or 50 ml methanol (for styrene) under vigorous stirring. The precipitated polymer was filtered with succion and dried in vacuum overnight.

3.2. Characterisation

3.2.1. Schiff base ligand *1-a*

Salicylaldehyde (0.24 g, 2 mmol), methylamine 2.0 M solution in THF (1 ml, 2 mmol) and THF (15 ml) afforded the compound as a yellow liquid: ^{1}H-NMR ($CDCl_3$) δ (ppm) 3.30 (s, 3H), 6.75–7.50 (m, 4H), 9.75 (s, 1H), 12.96 (s, 1H)); ^{13}C-NMR ($CDCl_3$) δ (ppm) 166.4, 161.7, 137.0, 133.8, 120.8, 119.9, 118.4, 45.9; IR (cm^{-1}) 3061, 2976, 2860, 2845–2910, 1623, 1573, 1525, 1497, 1465, 1125.

3.2.2. Schiff base ligand *1-b*

Salicylaldehyde (0.24 g, 2 mmol), *t*-butylamine (0.210 ml, 2 mmol) and THF (15 ml) afforded the compound as a yellow liquid: ^{1}H-NMR ($CDCl_3$) δ (ppm) 1.26 (s, 9H), 6.75–7.35 (m, 4H), 8.34 (s, 1H), 12.86 (s, 1H)); ^{13}C-NMR ($CDCl_3$) δ (ppm) 162.1, 159.6, 132.0, 131.3, 118.9, 118.1, 117.3, 56.9, 29.5; IR (cm^{-1}) 3031, 3061, 1626, 1572, 1522, 1497, 1464, 2840–2920, 1120.

3.2.3. Schiff base ligand *1-c*

Salicylaldehyde (0.24 g, 2 mmol), 4-bromo-2,6-dimethylaniline (0.4 g, 2 mmol) and ethanol (15 ml) afforded the compound as a yellow solid: ^{1}H-NMR ($CDCl_3$) δ (ppm) 2.21 (s, 6H), 7.15–7.30 (m, 6H), 8.32 (s, 1H), 12.85 (s, 1H); ^{13}C-NMR ($CDCl_3$) δ (ppm) 167.01, 160.92, 148.33, 138.99 133.35, 132.14, 130.79, 130.31, 118.97, 117.56, 117.22, 18.18; IR (cm^{-1}) 3031, 3065, 2850–2925, 1620, 1569, 1523, 1491, 1467, 1113.

3.2.4. Complex *3-a*

Ru dimer [$RuCl_2$(*p*-cymene)]$_2$ (0.49 g, 0.8 mmol), thallium salt **2-a** (0.54 g, 1.60 mmol), and THF (20 ml) afforded the complex **3-a** as a red-brown solid: ^{1}H-NMR ($CDCl_3$) aldimine ligand δ (ppm) 9.95 (s, 1H), 6.85–7.20 (m, 4H), 3.12 (s, 3H), *p*-cymene δ (ppm) 5.47 (d, 2H), 5.34 (d, 2H), 2.92 (sp, 1H), 2.17 (s, 3H), 1.25 (d, 6H); IR (cm^{-1}) 3050, 3032, 2956, 2923, 2853, 1920, 1672, 1594, 1536, 1467, 1447, 1376, 1347, 757; elemental analysis calculated (%) for $RuC_{18}H_{22}ONCl$ (404.90): C 53.40, H 5.48, N 3.46; found: C 53.34, H 5.44, N 3.44.

3.2.5. Complex *3-b*

Ru dimer [$RuCl_2$(*p*-cymene)]$_2$ (0.49 g, 0.8 mmol), thallium salt **2-b** (0.61 g, 1.60 mmol), and THF (20 ml) afforded the complex **3-b** as a red-brown solid: ^{1}H-NMR ($CDCl_3$) aldimine ligand δ (ppm) 8.25 (s, 1H), 6.85–7.00 (m, 4H), 7.26 (s, 2H) 2.54 (s, 6H), *p*-cymene δ 5.46 (d, 2H), 5.32 (d, 2H), 2.75 (sp, 1H), 2.24 (s, 3H), 1.25 (d, 6H); IR (cm^{-1}) 3052, 2962, 2918, 2851, 1933, 1732, 1606, 1528, 1462, 1443, 1379, 1361, 1261, 801; elemental analysis calculated (%) for $RuC_{21}H_{28}ONCl$ (446.98): C 56.43, H 6.31, N 3.13; found: C 56.38, H 6.33, N 3.16.

3.2.6. Complex *3-c*

Ru dimer [$RuCl_2$(*p*-cymene)]$_2$ (0.49 g, 0.8 mmol), thallium salt **2-c** (0.81 g, 1.60 mmol), and THF (20 ml) afforded the complex **3-c** as a red-brown solid. ^{1}H-NMR ($CDCl_3$) aldimine ligand δ (ppm) 9.85 (s, 1H), 6.83–7.10 (m, 4H), 1.35 (s, 9H), *p*-cymene δ (ppm) 5.48 (d, 2H), 5.36 (d, 2H), 2.90 (sp, 1H), 2.16 (s, 3H), 1.26 (d, 6H); IR (cm^{-1}) 3053, 2958, 2923, 2853, 1920, 1671, 1598, 1567, 1516, 1462, 1447, 1374, 757, elemental analysis calculated (%) for $RuC_{25}H_{27}ONClBr$ (573.92): C 52.32, H 4.74, N 2.44; found: C 52.22, H 4.78, N 2.41.

4. Conclusion

In conclusion, we succeeded in synthesising a new class of ruthenium-based catalysts which exhibit good activity in ATRP reactions. The ROMP activity of our systems for norbornene is poor but increases dramatically when TMSD is added to activate the catalytic systems. With the activated catalysts even the less strained cyclooctene can be converted smoothly. The results show that the control over polymerization is very dependent on the electronic and steric properties of the Schiff base ligands. So, by further fine-tuning the Schiff base ligands, the potential of these catalytic systems in the field of ROMP and ATRP can be much improved. Furthermore, the fact that these catalysts exhibit good activities in both ROMP and ATRP reactions allows them to combine the ROMP and the ATRP methodologies to make block copolymers with interesting properties by using new monomer combinations.

Further studies concerning these last two points are currently under investigation.

Acknowledgements

B.D.C. is indebted to the IWT (Vlaams instituut voor de bevordering van het wetenschappelijk-technologisch onderzoek in de industrie) for a research grant. F.V. is indebted to the Fund for Scientific Research-Flanders (Fonds voor Wetenschappelijk Onderzoek-Vlaanderen) and to the Research Council of Ghent University (Bijzonder Onderzoeksfonds) for financial support. M. Vandriessche (Texaco Research Centre, Ghent, Belgium) is gratefully acknowledged for the elemental analysis.

References

[1] O. Webster, Science 251 (1991) 887.
[2] K. Matyjaszewski, Cationic Polymerizations, Marcel Dekker, New York, 1996.
[3] (a) A.D. Jenkins, Macromoleculaire Chemie-Macromolecular Symposia 53 (1992) 267;
(b) R. Freitag, T. Baltes, M. Eggert, J. Polym. Sci. Part A: Polym. Chem. 32 (1994) 3019.
[4] (a) M. Kato, M. Kamigaito, M. Sawomoto, T. Higashimura, Macromolecules 28 (1995) 1721;
(b) M. Matsuyama, M. Kamigaito, M. Sawomoto, J. Polym. Sci. Part A: Polym. Chem. 34 (1996) 3585.
[5] (a) J.S. Wang, K. Matyjaszewski, J. Am. Chem. Soc. 117 (1995) 5614;
(b) J.S. Wang, K. Matyjaszewski, Macromolecules 28 (1995) 7901.
[6] (a) M. Sawomoto, M. Kamigaito, Chemtech 29 (1999) 30;
(b) K. Matyjaszewski, Chem. Eur. J. 5 (1999) 3095;
(c) K. Matyjaszewski, in: B. Marciniec (Ed.), Education in Advanced Chemistry, Mechanistic Aspects of Molecular Catalysis, Vol. 6, Wydawnictwo Poznanskie: Poznan-Wroclaw, 1999, pp. 95.
[7] (a) F. Simal, A. Demonceau, A.F. Noels, in: Proceedings of the 11th International Symposium on Homogeneous Catalysis (ISHC XI), University of St. Andrews, Scotland, UK, 12–17 July 1998;
(b) M.L. Snapper, J. Org. Chem. 64 (2) (1999) 344;
(c) A. Demonceau, F. Simal, A.F. Noels, in: Proceedings of the International Symposium on Romp and Related Chemistry-State of the Art and Visions for the New Century, Polanica-Zdroj, Poland, 3–15 September 2000.
[8] (a) K.J. Ivin, J.C. Mol, Olefin metathesis and metathesis polymerization, Academic Press, Cornwall, 1996, p. 476;
(b) T. Weskamp, F.J. Kohl, W. Hieringer, D. Gleich, W.A. Herrmann, Angew. Chem. Int. Ed. 38 (16) (1999) 2416;
(c) M. Scholl, T.M. Trnka, J.P. Morgan, R.H. Grubbs, Tetrahedron Lett. 40 (1999) 2247.
[9] A. Demonceau, A.W. Stumpf, E. Saive, A.F. Noels, Macromolecules 30 (1997) 3127.
[10] (a) T. Karlen, A. Ludi, A. Mühlebach, P. Bernhard, C. Pharisa, J. Polm. Sci. Part A: Polym. Chem. 33 (1995) 1665;
(b) A. Fürstner, L. Ackermann, J. Chem. Soc., Chem. Commun. (1999) 95.
[11] K. Matyjaszewski, JMS Pure Appl. Chem. A34 (10) (1997) 1785.
[12] Molecular Modelling was performed using PM3 methods (J. Stewart, J. Comput. Chem., 10 (1989) 221.) as implemented in SPARTAN (PC Spartan Plus, Wavefunction Inc., 18401 Van Karman Ave., Ste. 370, Irvine, CA 92612 USA).
[13] J.A.S. Howell, N.F. Ashford, D.T. Dixon, J.C. Kola, T.A. Albright, S.K. Kang, Organometallics 10 (1991) 1852.
[14] F. Simal, A. Demonceau, A. Noels, Angew. Chem. Int. Engl. Ed. 38 (1999) 538.
[15] M.A. Bennet, A.K. Smith, J. Chem. Soc., Dalton Trans. (1974) 233.